98-4570

APOLLO-DERIVED MARS PRECISION LANDER GUIDANCE

By

Gilbert L. Carman

Aerospace Engineer, Ascent/Descent Dynamics Branch, Flight Design and Dynamics Division
NASA Johnson Space Center, Houston, Texas

Dallas G. Ives

Aerospace Engineer, Advanced Mission Design Branch, Aeroscience and Flight Mechanics Division
NASA Johnson Space Center, Houston, Texas

David K. Geller

Charles Stark Draper Laboratory, Cambridge, Massachusetts

Abstract

The Earth entry guidance algorithm from the Apollo lunar program has been adapted as a candidate guidance algorithm for Mars precision landing missions. Although the original Apollo entry guidance had multiple phases to allow a wide range of entry velocity and ranging requirements, only the final entry phase of this algorithm is used for the Mars landing application. This phase utilizes bank angle to control range, based on deviations in range, altitude rate, and drag from a reference trajectory. An overview of the Apollo guidance, the modifications for Mars use, and the development of a Mars reference trajectory are given. The derivation of the control equation and gain computations are reviewed in detail. Impacts of the parachute deploy criteria upon guidance accuracy and target selection with respect to the vehicle maneuver capability envelope will be discussed. Results are presented for the Monte Carlo footprint resulting from expected dispersions using this algorithm with a preliminary 2001 Mars lander configuration as an example.

I. Introduction

The Mars Surveyor Program 2001 lander mission is currently scheduled for launch in April, 2001, and will perform a direct entry into the Martian atmosphere in January, 2002. The preliminary lander design is for an aeroshell configuration similar to Pathfinder, with a rover payload. The nominal total vehicle mass at entry interface is 523 kg. The trimmed lift to drag ratio was 0.18 for the cycle 1 vehicle configuration, and was later reduced to approximately 0.12 for the cycle 2 redesign work. An objective of the MSP '01 lander mission is a first demonstration of precision landing capability using active onboard entry guidance, in support of enhanced landing accuracy requirements of future robotics missions and subsequent manned landings. The goal of the MSP '01 precision landing demonstration is to achieve parachute deployment within a horizontal 10 km radius of the nominal target. Terminal phase deceleration will be accomplished by the parachutes, followed by powered descent to a soft landing using a hydrazine monopropellant system and landing radar.

At the first MSP '01 Atmospheric Flight Team Meeting in August, 1997, the Apollo command module entry guidance was proposed as a candidate algorithm which could be adapted for use with the Mars 2001 lander. The Apollo guidance has been man rated and successfully flight proven with the 0.3 L/D command module on entries from Earth orbit as well as direct lunar returns. A detailed development of all phases of the Apollo guidance algorithm and their application to Apollo Earth entry trajectories is presented in Reference 2. The objective of this paper is to present

the modifications which have been made to adapt this algorithm for use with Mars entry trajectories.

II. Guidance overview

The original Apollo guidance design was for lunar return; however, sufficient mission flexibility was required to accommodate the large variations in entry conditions encountered, including those of Earth orbit test flights and all types of lunar mission aborts. To achieve adequate performance for the relatively shallow initial flight path angles and low load factor limits of the manned Apollo entries, an upper altitude controlled skipout capability was included. This skipout control consisted of Huntest, Down control, Up control, and Kepler phases, which were designed to set up desired initial conditions for the final phase entry. Figure 1 shows an overview of these guidance phases. Since the MSP '01 lander trajectory will be targeted for a much steeper entry interface than the Apollo lunar returns, the skipout control phases are not invoked, and only the second entry phase is used. The second entry final phase algorithm controls to a fixed reference trajectory, consisting of range to go, drag acceleration, and altitude rate as a function of relative velocity. A constant initial prebank attitude is maintained until a sensed atmospheric drag acceleration of 0.05 Earth g's, when closed loop guidance bank commands are initiated.

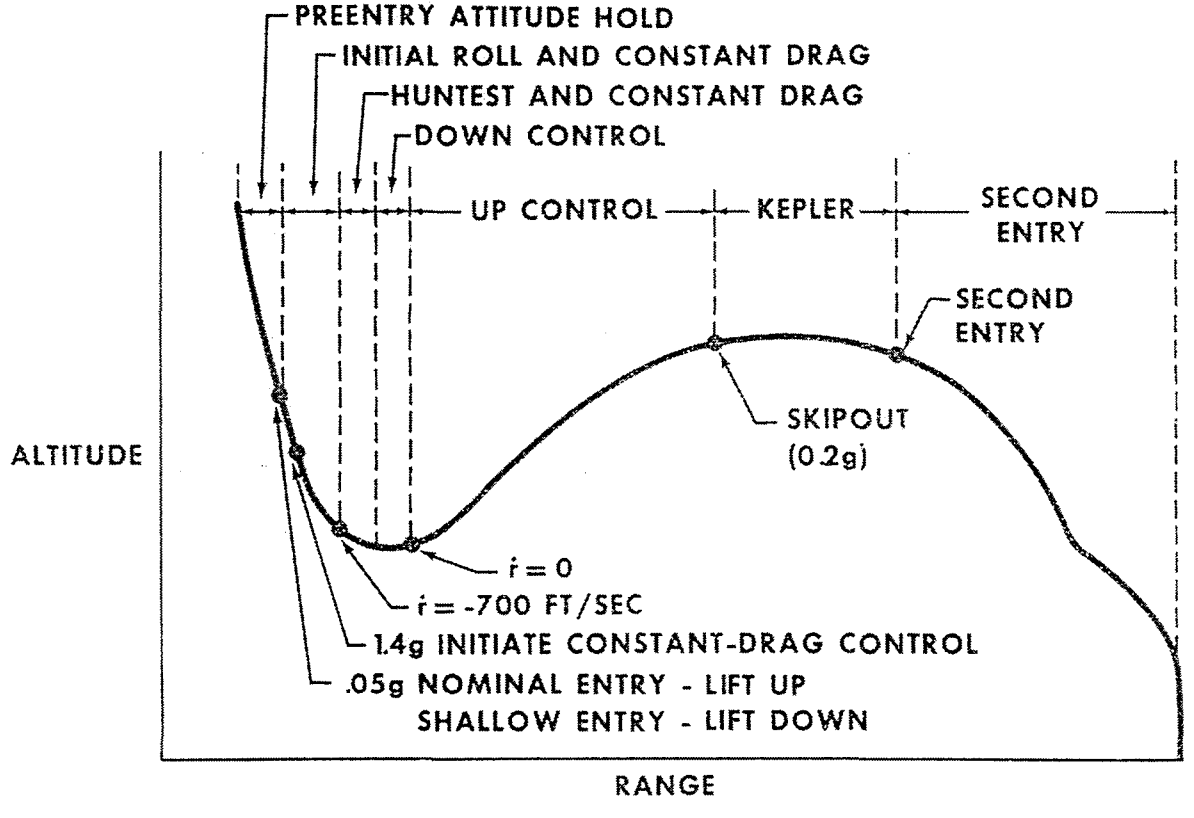

Figure 1. Apollo entry guidance phases

The predicted range to go is calculated as a function of drag and altitude rate errors with respect to the nominal reference trajectory profile, as in equation 1.

$$R_p = R_{ref} + \frac{\partial R}{\partial D}\left(D - D_{ref}\right) - \frac{\partial R}{\partial \dot{r}}\left(\dot{r} - \dot{r}_{ref}\right) \qquad (1)$$

The desired vertical component of the lift to drag ratio is calculated as a function of the difference between the actual and predicted range to go.

$$\left(\frac{L}{D}\right)_C = \left(\frac{L}{D}\right)_{ref} + \frac{K_3\left(R - R_p\right)}{\partial R / \partial\left(L/D\right)} \qquad (2)$$

The commanded bank angle is then calculated as

$$\Phi_C = \cos^{-1}\left(\frac{L/D_C}{L/D}\right) * K2ROLL \qquad (3)$$

The partial derivatives of predicted range in equations 1 and 2 are the controller gains, which are derived using linear perturbation theory with the nominal reference trajectory by reverse integration of the differential equations which are adjoint to the linearized equations of motion. Appendix A presents a detailed development of these derivations. F_1, F_2, and F_3 (equations 23-25 of appendix A) are the optimized control gains for converging the dispersed trajectory to the nominal reference at final velocity, and are implemented in the guidance as tabular functions of relative velocity. Because of slow system and trajectory responses to guidance commands, performance is empirically improved by the use of the over control gain K_3 in equation 2 to achieve convergence prior to final velocity. The sensed drag acceleration and lift to drag ratio (*D* in equation 1 and *L/D* in equation 3) are derived from accelerometer measurements and smoothed by first order filters with a one second time constant. The term *K2ROLL* in equation 3 is the bank directional control (±1), which is reversed each time the target crossrange out of plane central angle exceeds the reversal criterion, which is a quadratic function of relative velocity.

III. Reference profile design and target selection

There are only four planetary physical constants used by the Apollo final phase algorithm which required updating for Mars. For guidance development and evaluation work, the MSP '01 initial entry conditions were the same for all candidate guidance algorithms, and each developer defined his own parachute deploy target, consistent with the design requirements of each algorithm. Since the objective of the Apollo guidance is to acquire and maintain a fixed reference trajectory profile, it is desirable that this profile be designed to provide as much margin as possible from the vehicle maneuver capability limits to accommodate dispersions. The primary objective of the cycle 1 lander guidance design was to achieve the best horizontal position accuracy possible with respect to the desired parachute deploy target, with no constraining criteria on final altitude or dynamic pressure. The initial step in selection of the optimum reference trajectory and parachute deploy target was to determine the maximum vehicle maneuver capability for the planned initial conditions. A series of nominal unguided constant bank angle entry simulations were performed to define the open loop maneuver capability envelope at parachute deploy. This envelope is shown in figure 2 for the parachute deploy criterion of 503.8 meters per second navigated relative velocity, and represents the deploy target positions which can be achieved for the nominal undispersed MSP '01 environment and vehicle L/D values of 0.18 and 0.12. Since the effects of the majority of the dispersion sources are symmetric about their means, the guidance ability to achieve the desired target in the presence of dispersed environments and system errors is maximized by shaping the nominal reference trajectory profile to target the center of the above maneuver capability. For the MSP '01 cycle 1 configuration and nominal environment, this was found to be a constant bank angle trajectory of 53 deg with a single reversal to null the terminal crossrange error, which resulted in a guidance parachute deploy position target which was approximately 87 km downrange of the zero lift ballistic impact point. Controller gains were then derived, based on this reference trajectory.

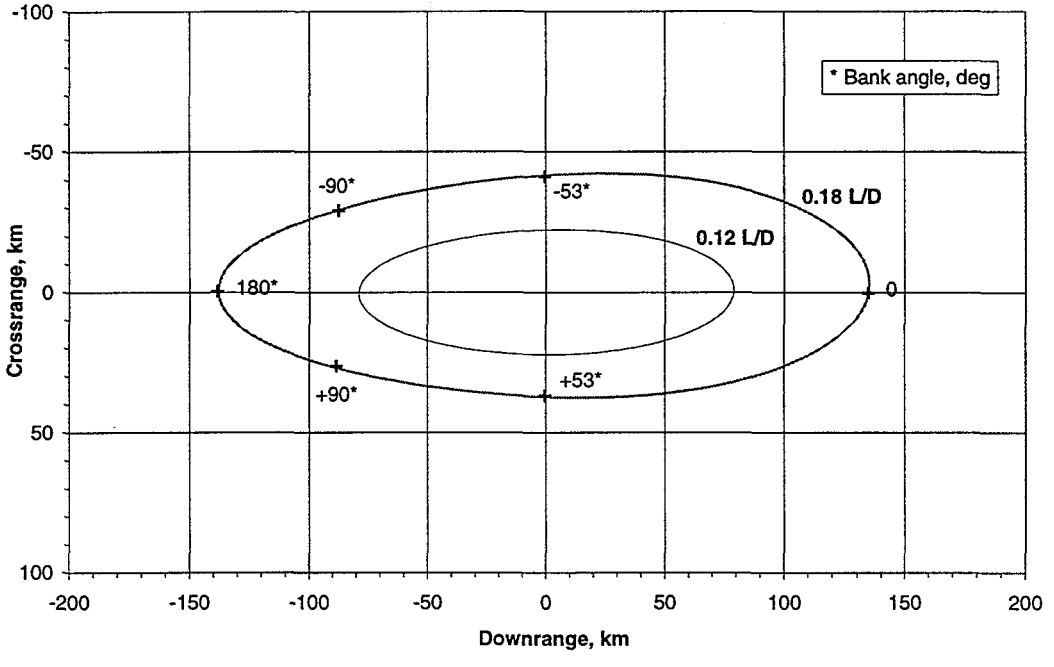

Figure 2. MSP '01 Nominal constant bank maneuver capability

IV. Drag control tuning

Early performance results for dispersed cases showed slow and overdamped response characteristics in acquiring and maintaining the reference drag profile late in the trajectory. This slow response is due primarily to the low atmospheric density, vehicle lift to drag ratio, and roll acceleration, compared to Apollo command module Earth entries. Atmospheric density dispersion is the principal factor which degrades the guidance ability to maintain a fixed drag versus velocity profile. In order to compensate for off nominal density dispersions, the geometric altitude must vary in an attempt to maintain nominal density altitudes. The purpose of the altitude rate error term in the ranging equation is to provide control damping to prevent excessive overshoot and oscillation in drag error convergence response characteristics. The altitude rate gain decreases to zero at final velocity, so drag error is the principal contributor to target miss. In the presence of off nominal atmospheric density, the altitude and altitude rate must deviate from nominal to achieve an acceptable convergence of drag error. A significant improvement in drag error convergence was achieved by reducing the altitude rate gain as a function of drag error, resulting in smaller target miss distances. This gain compensation has the effect of changing the balance of the over control gain K_3 to achieve improved drag control by reducing the system damping, allowing larger altitude rate deviations and faster convergence of drag errors.

V. Lateral control tuning

The initial bank command at guidance start is in the direction of the target position with respect to the relative trajectory plane. Bank reversals are triggered when the magnitude of the target crossrange out of plane central angle exceeds the reversal criterion, which is a quadratic function of relative velocity. Dispersions in atmospheric density can result in bank angle commands which remain saturated at maximum

or minimum limits for a significant length of time, slowing the convergence of crossrange error. The original Apollo guidance utilized only a single crossrange corridor. However, as a result of the larger atmospheric density variations and smaller vehicle lift to drag ratio of MSP '01, compared to Apollo, a tighter crossrange corridor was added prior to the first bank reversal, which provides improved performance by minimizing the peak crossrange overshoot which occurs after the first reversal. The corridor width is increased to the second level when the first reversal is initiated.

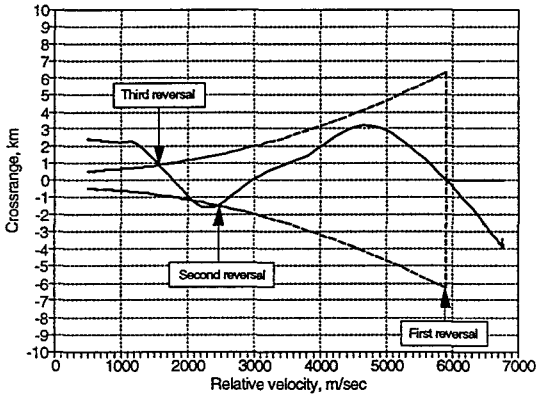

Figure 3. Bank reversal corridor

Bank reversals are inhibited at relative velocities less than 3000 ft/sec (914 m/sec) to prevent excessive lofting or drooping effects late in the trajectory. This was found to produce the best compromise between the degradation in downrange control which would result from late reversals near the target and the larger crossrange errors which would be produced by inhibiting reversals too early. Dual minimum bank angle command limits (maximum cosine limits) were also implemented to maintain adequate crossrange control capability when the vertical *L/D* commands are large. The minimum bank limit is normally 15 deg, but is increased to 30 deg when crossrange error exceeds 200% of the reversal corridor.

VI. Cycle 1 performance results

A disadvantage of using discrete bank reversals to control crossrange, as in the Apollo guidance, is the loss of closed loop drag and altitude rate control during the period of time that the reversal is in progress. For optimum ranging control, the number of reversals must, therefore, be minimized, consistent with preserving acceptable crossrange control. The time required to perform the bank reversals is a function of the magnitude of the required change in bank angle and the roll axis response of the flight control system. The lifting trajectory design provides good drag control and parachute deploy position accuracy because of the relatively long range and total flight time. The low bank angles also result in shorter duration bank reversals, so there is not as much loss of drag control as there would be with a steeper and shorter range trajectory which would require larger average bank angles. The nominal dynamic pressure at parachute deploy is approximately 350 nt/m^2 for this profile. Figure 4 below shows the parachute deploy conditions that were achieved with the shallow profile design for 100 Monte Carlo 3 degree of freedom dispersed entry simulations.

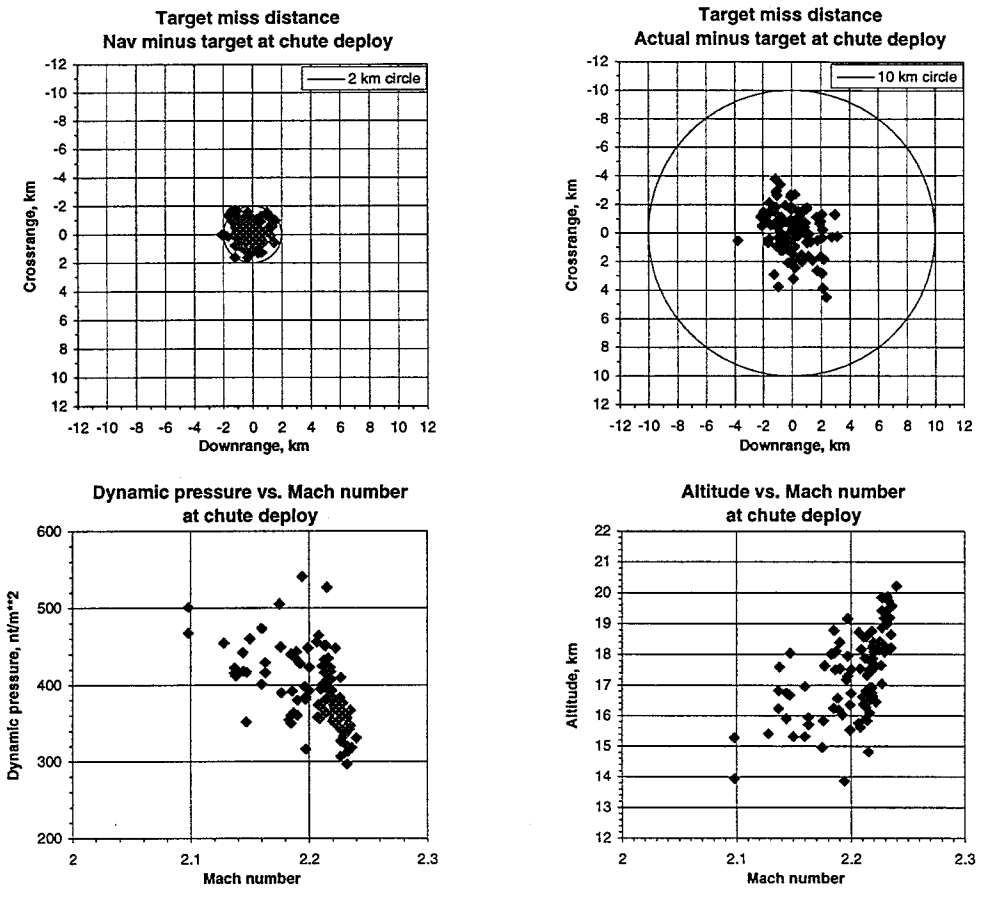

Figure 4. Shallow profile parachute deploy results (100 3DOF cases)

The maximum horizontal position miss distances with respect to the desired parachute deploy target were 2.2 km for the navigated state and 5.1 km for the actual state. Since the guidance steering commands are based on the navigated state vector, the navigated position minus target position at parachute deploy is the best indicator of guidance accuracy performance. Errors in navigated position with respect to the actual state are unknown to the guidance, and will add to the actual state miss distances. Error in the horizontal component of the navigation system's knowledge of position at parachute deploy was as large as 4.9 km in some cases, and was the largest contributor to the actual position miss distances. Any additional horizontal drift from parachute deploy until final touchdown is not included in these simulations. These shallow profile results are based on the cycle 1 mission configuration, which was targeted for an equatorial landing near 150 deg east longitude.

VII. Parachute deploy constraints

As a result of mission configuration updates, additional parachute deploy requirements were imposed for the cycle 2 redesign which were incompatible with the optimized cycle 1 shallow reference trajectory. Minimum and maximum constraints for Mach number and dynamic pressure for the cycle 2 redesign were 1.3 to 2.3 and 400 to 1300 nt/m^2, respectively. Since these dynamic pressure constraints are based on design specifications for the Pathfinder zero lift ballistic trajectory, they are higher than can be obtained with a lifting trajectory. Therefore, the Apollo '01 design was changed to a near zero lift reference (87 deg nominal bank angle), in order to achieve the required low altitude and high dynamic pressure deploy conditions for which the parachutes were designed. Maximum and minimum navigated altitude constraints of 13.5 km and 6.5 km, respectively, were also added to the parachute deploy requirements to indirectly protect against low altitude potential impact cases. Parachute

deploy will occur at a navigated relative velocity of 503.8 m/sec if the altitude is within limits. However, if a navigated altitude of 6.5 km occurs prior to 503.8 m/sec, parachute deploy will occur at that time. Cases in which the navigated altitude exceeds 13.5 km at 503.8 m/sec will have parachute deploy delayed until 13.5 km navigated altitude. These additional altitude criteria contribute to larger target miss distances for cases which have large navigation errors in altitude, but provide protection against potential surface impact cases. Figure 5 shows the dynamic pressure vs. Mach number corridor for the nominal MSP '01 atmosphere and no winds. As can be seen from this data, it was not possible to meet the above parachute deploy requirements with the cycle 1 shallow trajectory design.

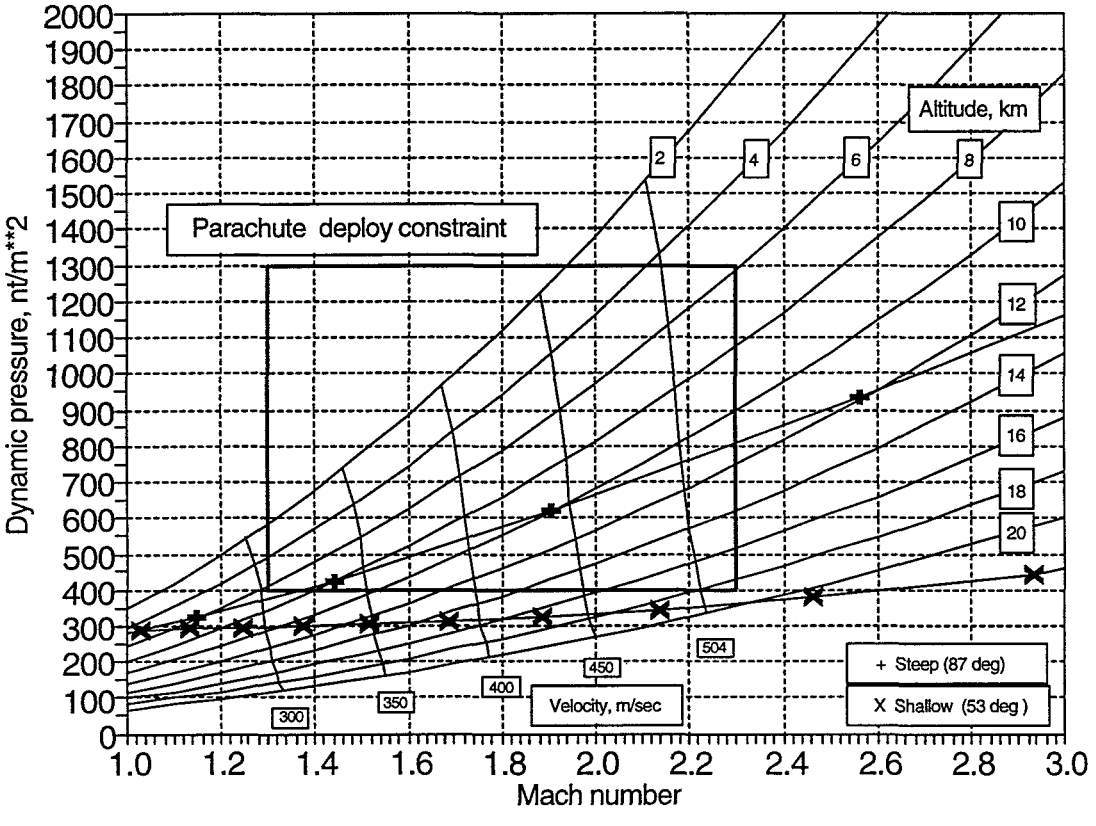

Figure 5. Dynamic pressure vs. Mach number corridor

To minimize the number of dispersed cases which have parachute deploy at off nominal velocities as a result of final navigated altitude constraints, the revised cycle 2 trajectory profile was designed to achieve the nominal parachute deploy velocity of 503.8 m/sec at an altitude of 10 km in the presence of average winds, which is the center of the allowable corridor. This redesign to a steep reference trajectory resulted in a significant degradation in guidance accuracy capability because the total flight time of the steeper short range profile is reduced to approximately half that of the shallow trajectory, and the larger bank angles result in longer duration bank reversals.

As a result of the shorter flight time available to converge trajectory errors, the bank reversal corridor had to be reduced to smaller values than with the shallow profile, and a prebank maneuver to 45 deg was added to reduce the time required to achieve the initial bank commands at the start of closed loop drag control. Since there is no closed loop guidance control for the duration of the bank reversals, the lofting or drooping

effects on the trajectory which result from reversals either over the top or under the bottom, respectively, must be minimized. With the shallow lifting trajectory design, reversals over the top are always preferred, and bank angle limits of ±70 deg were used until a relative velocity of 8000 ft/sec (2438 m/sec). Below 8000 ft/sec, bank angle commands up to ±180 deg were allowed. However, with the steeper zero lift trajectory, a large percentage of cases showed a significant improvement in performance if the bank reversal maneuvers are performed under the bottom. The reversal direction criterion which produced the best results was the magnitude of the commanded bank angle at the time of the reversal. For relative velocities greater than 10,000 ft/sec (3048 m/sec), reversals are performed over the top if the bank angle command is less than 170 deg and under the bottom if greater than 170 deg. Below 10,000 ft/sec, this criteria is changed to 100 deg.

The altitude rate gain compensation described earlier with the cycle 1 shallow profile was designed to allow larger altitude deviations to achieve improved drag control. However, with the addition of altitude constraints on parachute deploy, it is more desirable to reduce altitude deviations late in the trajectory. This was accomplished empirically with a 50% reduction in the drag controller gains for velocities below 5000 ft/sec (1524 m/sec). This compensation results in less altitude deviation from the reference profile at the expense of slightly larger drag errors. Figure 6 shows the best parachute deploy conditions obtained with the cycle 2 steep trajectory design for the 100 dispersed 3 degree of freedom Monte Carlo cases that were analyzed. The maximum target miss distances for this set of cases were 6.2 km navigated and 10.1 km actual. The cycle 2 mission configuration was based on a target landing site of 15.2 deg north latitude and 96 deg west longitude, which resulted in navigated horizontal position knowledge errors as large as 9.6 km for the above cases, which was more than twice as large as with the cycle 1 design. Results of 2000 dispersed cases for both 3 and 6 degree of freedom simulations are presented on pages 10-13. Horizontal errors in the navigation system's knowledge of position at parachute deploy for this increased sample size was as large as 15.8 km in some cases.

VIII. Conclusions

The Apollo entry guidance has been demonstrated to be adaptable for use with the Mars 2001 lander configuration and environment. The simplicity of this single phase guidance implementation results in relatively low computer resource requirements. Optimum accuracy results can be obtained with a lifting reference trajectory design; however, current parachute deployment constraints require targeting for a non optimum zero lift trajectory. The dominate factor in parachute deployment position accuracy capability is error in the onboard navigated state vector.

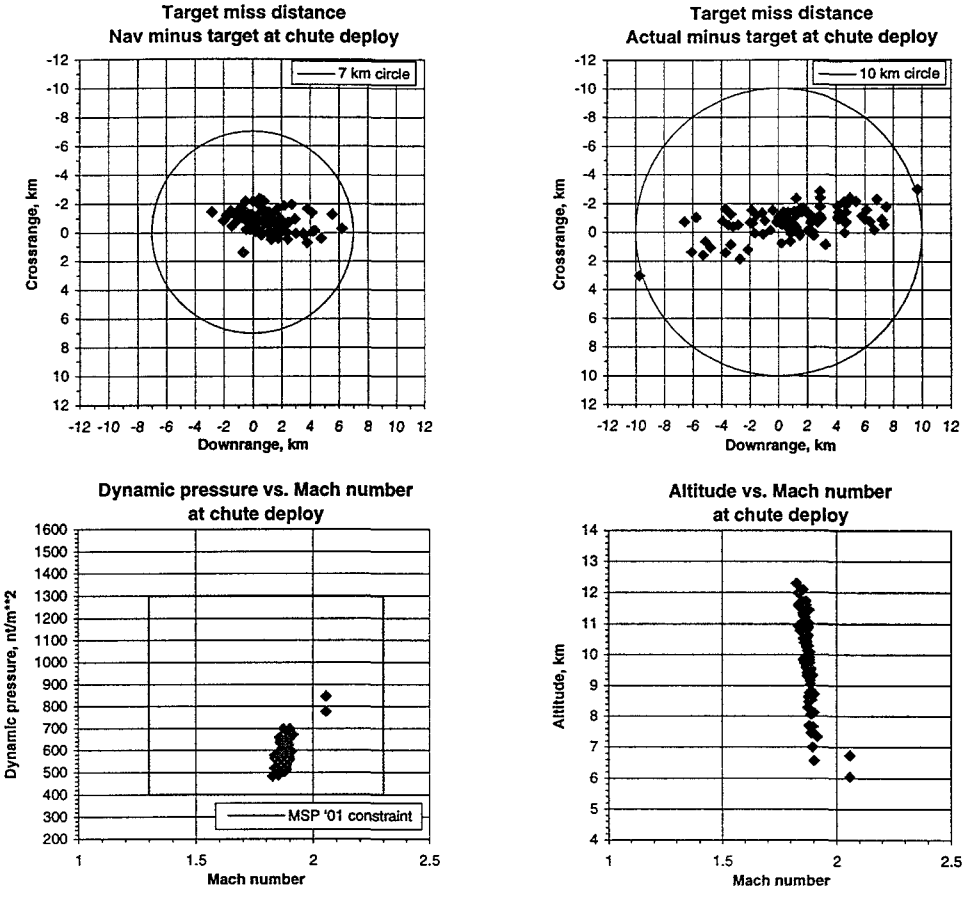

Figure 6. Steep profile parachute deploy results (100 3DOF cases)

Apollo Guidance: 3DOF Lander Simulation Results

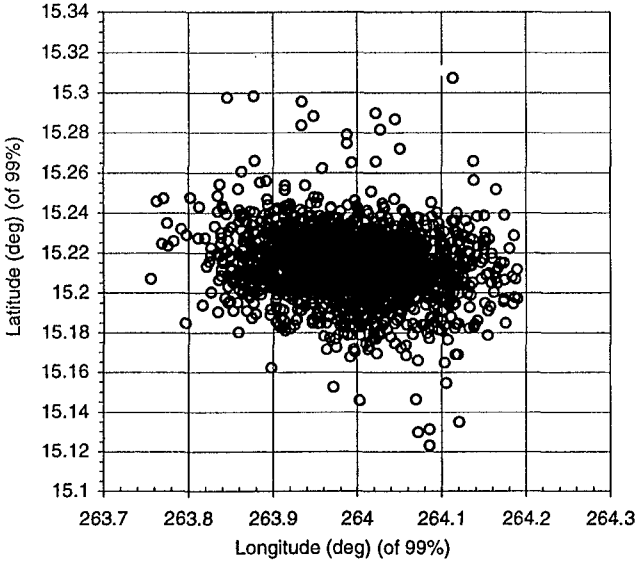

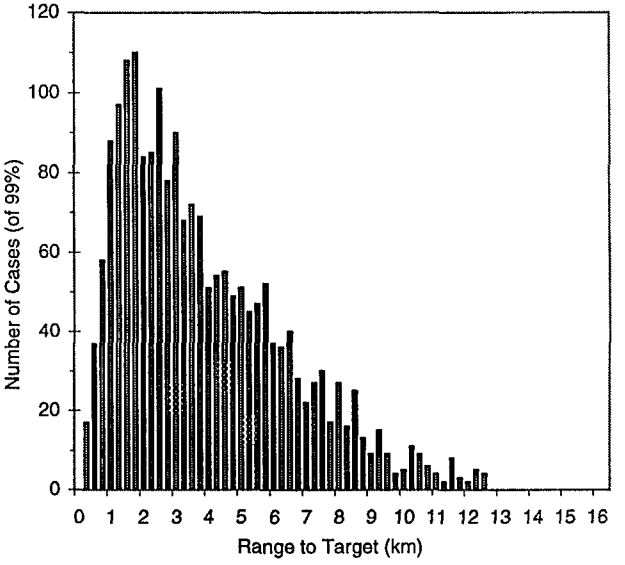

99.0 % range between	0.05	and	12.41	km
96.3 % less than 10 km				
These cases are characterized by:				
Alt at chute deploy of	5.2	to	13.4	km
Dynamic pressure of	415.4	to	979.7	nt/m ^{2}
Mach number of	1.68	to	2.24	
Flight Path Angle of	-29.43	to	-10.37	deg
Heat Rate of	82.7	to	99.9	W/cm ^{2}
Total Heat Load of	2977	to	3252	J/cm ^{2}
Peak g Load of	14.0	to	20.3	g

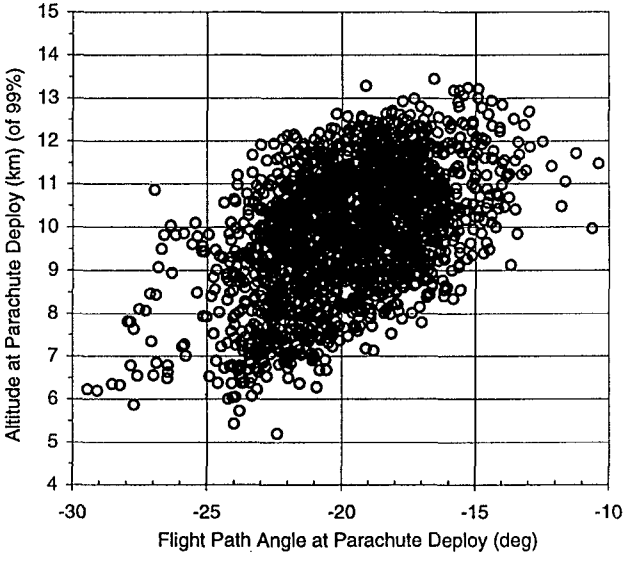

Apollo Guidance: 3DOF Lander Simulation Results

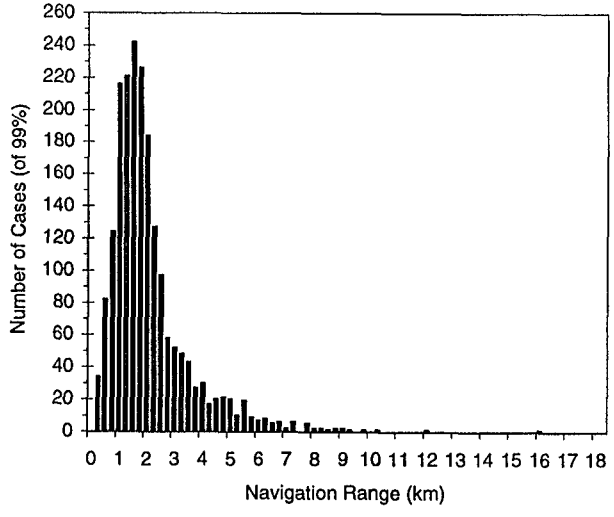

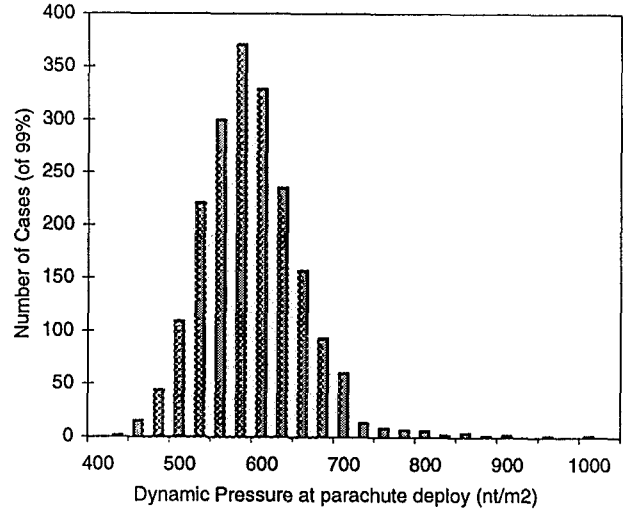

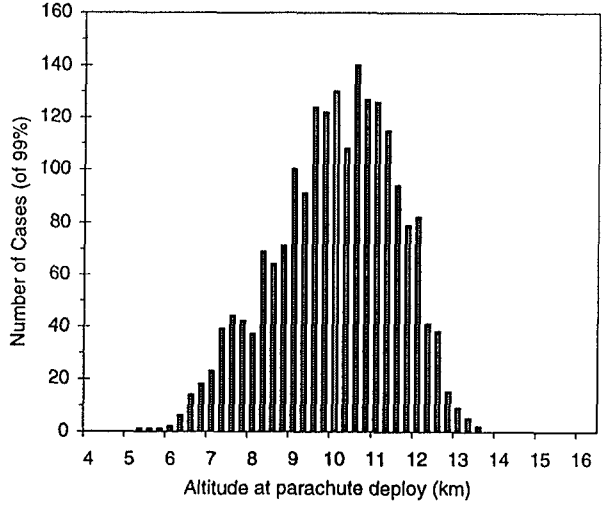

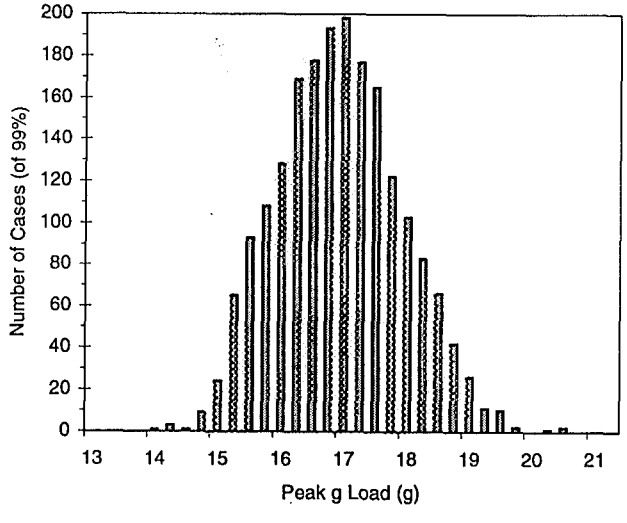

Apollo Guidance: 6DOF Lander Simulation Results

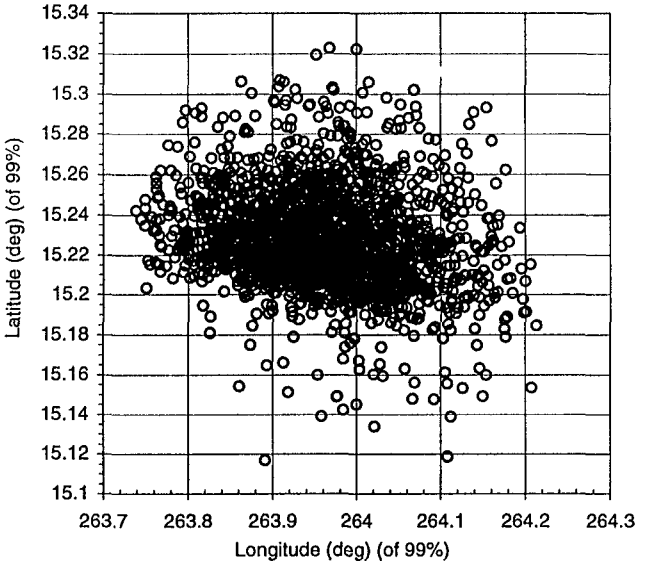

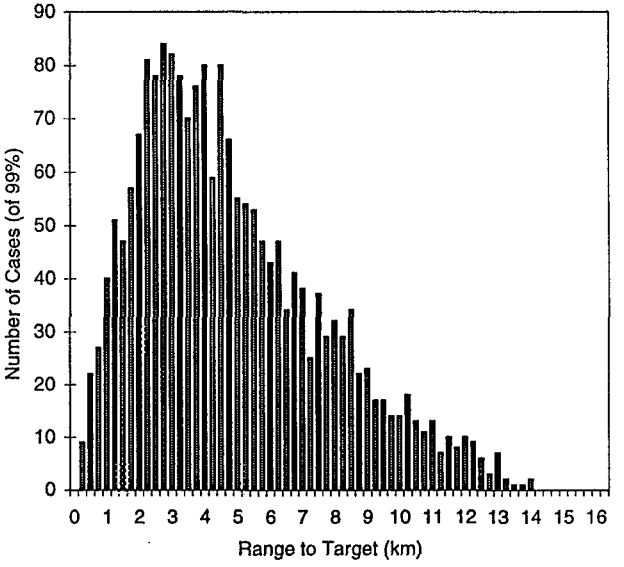

99.0 % range between	0.01	and	13.81	km
93.0 % less than 10 km				
These cases are characterized by:				
Alt at chute deploy of	6.0	to	13.3	km
Dynamic pressure of	400.3	to	902.9	nt/m ^{2}
Mach number of	1.67	to	2.22	
Flight Path Angle of	-25.29	to	-12.79	deg
Heat Rate of	80.8	to	101.4	W/cm ^{2}
Total Heat Load of	2941	to	3184	J/cm ^{2}
Peak g Load of	13.8	to	19.9	g
RCS Propellant of	1.29	to	3.02	kg

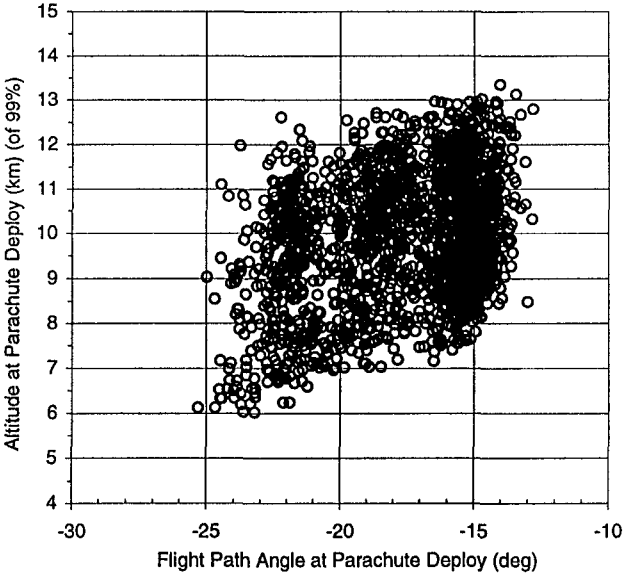

Apollo Guidance: 6DOF Lander Simulation Results

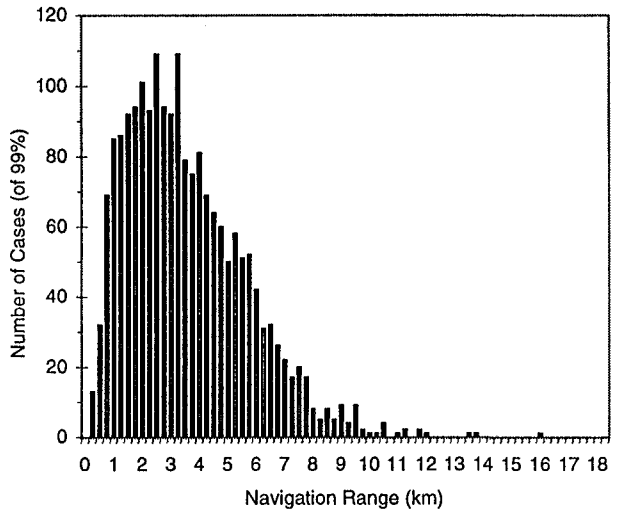

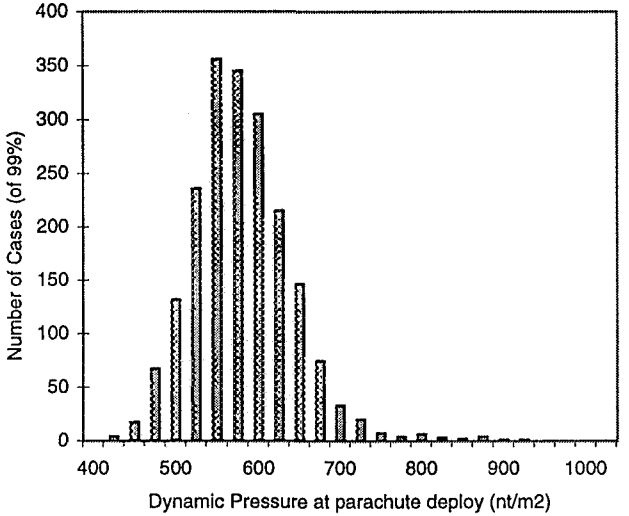

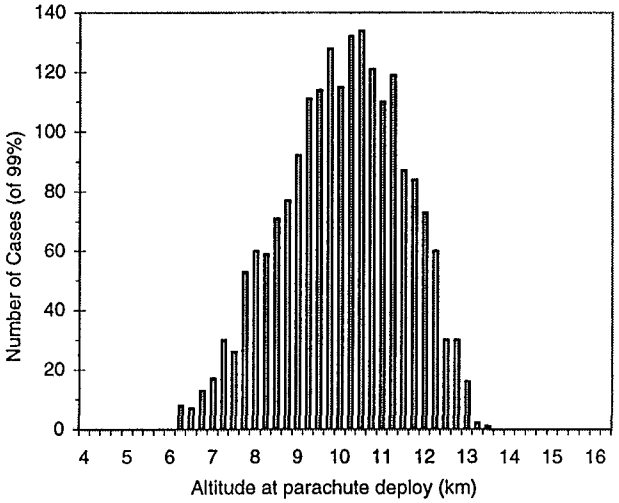

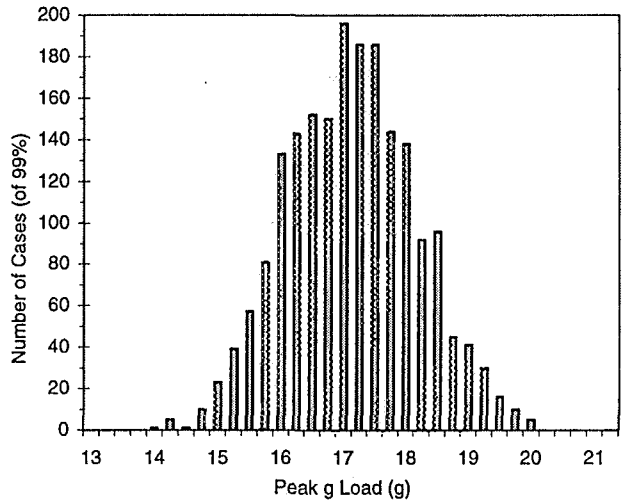

Appendix A. - Control Law Gain Derivation

This appendix presents the methodology that was used to derive the gains for the Apollo Guidance control law.

Theoretical Development - The in-plane equations of motion associated with atmospheric flight can be written approximately as:

$$\frac{ds}{dt} = v\cos\gamma \tag{1}$$

$$\frac{dv}{dt} = -\left(\frac{D}{m} + g_s \sin\gamma\right) \tag{2}$$

$$\frac{d\gamma}{dt} = \frac{L\cos\phi}{mv} + \left(\frac{v}{r_e + h} - \frac{g_s}{v}\right)\cos\gamma \tag{3}$$

$$\frac{dh}{dt} = v\sin\gamma \tag{4}$$

where $s(t)$ is range, $v(t)$ is relative velocity, $\gamma(t)$ is the relative flight path angle, $h(t)$ is altitude, ϕ is the bank angle, m is the mass of the vehicle, r_e is the planet equatorial radius, and g_s is the gravitational acceleration at the surface. The lift, L, and drag, D, are assumed to be given by:

$$L = qC_L A_{rea}, \quad D = qC_D A_{rea} \tag{5}$$

where $q=\rho(h)v^2/2$ is the dynamic pressure, and $\rho(h)=\rho_o \exp[-h/h_s(h)]$ is the atmospheric density. By defining a state vector, $x(t)=[s(t), v(t), \gamma(t), h(t)]^T$, Eqs. 1-4 can be written in the compact form:

$$\frac{dx}{dt} = f(x, u) \tag{6}$$

where the control u is $u=(L/D)\cos\phi$. For a given bank angle profile, a nominal reference trajectory, $x^*(t)=[s^*(t), v^*(t), \gamma^*(t), h^*(t)]^T$, is easily determined by integrating Eqs. 1-4 (or Eq. 6) forward from a nominal set of initial conditions, $x_0 = \left[s_0^*, v_0^*, \gamma_0^*, h_0^*\right]^T$.

A standard procedure used to determine the effect of *small* state and/or control perturbations on the final range error is to linearize the dynamic equations of motion about the nominal trajectory,

$$\frac{d(\delta x)}{dt} = \left(\frac{\delta f}{\delta x}\right)_{x^*,u^*} \delta x(t) + \left(\frac{\delta f}{\partial u}\right)_{x^*,u^*} \delta u \tag{7}$$

where the indicated derivatives are evaluated along the nominal trajectory. At any given time, t, the effect of the state perturbation, $\delta x(t)=x(t)-x^*(t)=[\delta s(t), \delta v(t), \delta\gamma(t), \delta h(t)]^T$, on the final range error is given by:

$$\delta R_f = \lambda(t) \cdot \delta x(t) \tag{8}$$

where $\lambda(t) = \left[\lambda_s(t), \lambda_v(t), \lambda_\gamma(t), \lambda_h(t)\right]^T$ is a vector of influence coefficients that must

satisfy the system of differential equations *adjoint* to Eq. 7,

$$\frac{d\lambda}{dt} = -\left(\frac{\delta f}{\delta x}\right)^T_{x^*,u^*} \lambda(t) \tag{9}$$

with the boundary condition:

$$\lambda_f^T = \frac{\partial \delta R_f}{\partial \delta x_f} \tag{10}$$

The final range (see Fig. 1) can be determined geometrically as:

$$\begin{aligned} R_f &= s_f + \dot{s}_f \, dt_f \\ &= s_f + \frac{\dot{s}_f}{\dot{h}_f} h_f \end{aligned}$$

Substituting in Eqs. 1 and 4 gives:

$$R_f = \delta s_f - \frac{\cos\gamma_f}{\sin\gamma_f} \delta h_f$$

the boundary conditions in Eq. 10 must be

$$\begin{aligned} &\lambda_s(t_f) = 1, \qquad \lambda_v\left(t_f\right) = 0 \\ &\lambda_\gamma\left(t_f\right) = 0, \qquad \lambda_h\left(t_f\right) = -\cot\left(\gamma_f^*\right) \end{aligned}$$

By integrating the adjoint equations (Eq. 9) backward from time t_f to a time t using the above boundary conditions, we obtain $\lambda(t)$, which can then be used to predict the final range error given by Eq. 8.

$$\delta R_f = \lambda_s(t)\delta s(t) + \lambda_v(t)\delta v(t) + \lambda_\gamma(t)\delta\gamma(t) + \lambda_h(t)\delta h(t) \tag{11}$$

Changing the independent variable to v and the dependent variables δh, $\delta\gamma$ to $\delta(D/m), \delta\dot{h}$ produces the final result,

$$\delta R_f = \lambda_s(v)\delta s(v) + \frac{\lambda_\gamma^*(v)}{v\cos\gamma(v)} \delta\dot{h}(v) - \frac{m h_s^*(v)\lambda_h(v)}{D^*(v)} \delta[D(v)/m]. \tag{12}$$

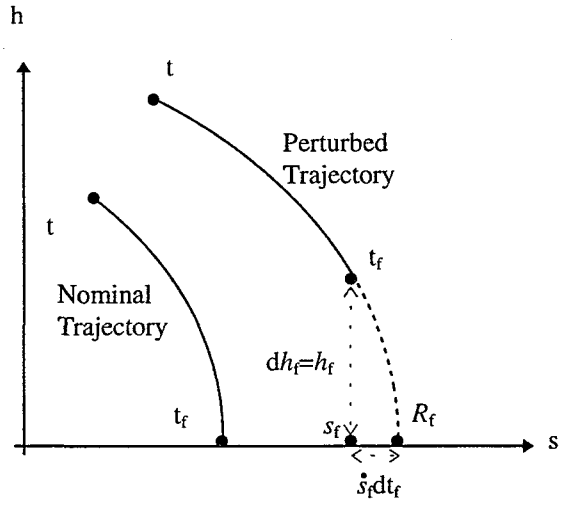

Figure 1.0

The next step is to determine a correction to the control that will null out the predicted final range error. If we assume that the control correction δu is constant, the solution to the linearized equations of motion in Eq. 7 is

$$\delta x_f = \Phi(t_f,t)x(t) + \left[\int_t^{t_f} \Phi(t_f,\tau)B(\tau)d\tau\right]\delta u \tag{13}$$

where $\Phi(\cdot,\cdot)$ is the state transition matrix, and $B(\tau) = [0,0,D^*/mv^*,0]^T$. The final range error associated with δx_f is $\delta R_f = \lambda_f \cdot \delta x_f$ (see Eq. 8). Substituting Eq. 13 for δx_f, and taking the partial of δR_f with respect to the control δu gives

$$\lambda_u(t) = \frac{\partial \delta R_f}{\partial \delta u} = \int_t^{t_f} \lambda_f \Phi(t_f,\tau)B(\tau)d\tau \tag{14}$$

Clearly, $\lambda_u(t_f) = 0$, and taking the time derivative of Eq. 14 produces

$$\frac{d\lambda_u}{dt} = -B(t)\cdot\lambda(t) = \frac{-D^*}{mv^*}\lambda_\gamma(t) \tag{15}$$

Integrating Eq. 15 backward from time t_f to a time t using the boundary condition $\lambda_u(t_f) = 0$ will provide $\lambda_u(t)$, and the control correction required to null the final range error δR_f is then given by

$$\delta u = \frac{-\delta R_f}{\lambda_u(t)}. \tag{16}$$

Changing the independent variable in the above expression to v, and substituting Eq. 12 into 16 produces the feedback control law:

$$u = u^* + \frac{1}{\lambda_u(v)}\left[\lambda_s(v)\delta s + \frac{\lambda_\gamma(v)}{v\cos\gamma^*(v)}\delta h(v) - \frac{mh_s^*(v)\lambda_h(v)}{D^*(v)}\delta\left(D(v)/m\right)\right] \tag{17}$$

Implementation - First, calculate a nominal reference trajectory $x^*(t) = \left[s^*(t), v^*(t), \gamma^*(t), h^*(t)\right]^T$ by integrating $\dot{s}, \dot{v}, \dot{\gamma}, and\ \dot{h}$ forward from an appropriate set of initial conditions using Eqs. 1-4. In practice this was done by using an existing trajectory program (POST) to calculate the reference trajectory as discussed in Section III. Next calculate the control law gains by integrating the adjoint equations backwards along the nominal reference trajectory from t_f to the initial time t_o. The adjoint equations (see Eq. 9) are given by:

$$\frac{d\lambda_s}{dt} = 0 \tag{18}$$

$$\frac{d\lambda_v}{dt} = -\cos\gamma^*\lambda_s(t) + \left(\frac{\rho^* v^* C_D A_{rea}}{m}\right)\lambda_v(t) + \tag{19}$$
$$+\left(\frac{\rho^* C_L \cos(\Phi) A_{rea}}{2m} + \frac{\cos\gamma^*}{r_e + h^*} + \frac{g_s\cos\gamma^*}{(v^*)^2}\right)\lambda_\gamma(t) - \sin\gamma^*\lambda_h(t)$$

$$\frac{d\lambda_\gamma}{dt} = v^*\sin\gamma^*\lambda_s(t) + g_s\cos\gamma^*\lambda_v(t) + \tag{20}$$
$$+\left[\left(\frac{v^*}{r_e + h^*} - \frac{g_s}{v^*}\right)\sin\gamma^*\right]\lambda_\gamma(t) - v^*\cos\gamma^*\lambda_h(t)$$

$$\frac{d\lambda_h}{dt} = \left(\frac{-D^*/m}{h_s^*}\right)\lambda_v(t) + \left(\frac{L^*\cos(\Phi)/m}{h_s^* v^*} + \frac{v^*\cos\gamma^*}{(r_e + h^*)^2}\right)\lambda_\gamma(t) \tag{21}$$

$$\frac{d\lambda_u}{dt} = \left(\frac{-D^*/m}{v^*}\right)\lambda_\gamma(t) \tag{22}$$

and the boundary conditions are

$$\lambda_s(t_f) = 1, \qquad \lambda_v(t_f) = 0$$
$$\lambda_\gamma(t_f) = 0, \qquad \lambda_h(t_f) = -\cot(\gamma_f^*)$$

Next, calculate and save the following gains as a function of v.

$$F_1(v) = -\frac{mh_s^*(v)}{D^*(v)}\lambda_h(v) \tag{23}$$

$$F_2(v) = \frac{\lambda_\gamma(v)}{v\cos\gamma^*(v)} \tag{24}$$

$$F_3(v) = \lambda_u(v) \tag{25}$$

Using the above gains, the final control law takes the form

$$(L/D)\cos\phi = (L/D)^{*}\cos\phi^{*} + \frac{K}{F_3(v)}\left[-\left(s - s^{*}(v)\right) - F_2(v)\left(\dot{h} - \dot{h}^{*}(v)\right) + F_1(v)\left(D/m - D^{*}(v)/m\right)\right] \quad (26)$$

where

$$s - s^{*} = -(PredRangeToGo - NomRangeToGo(v)), \quad (27)$$

and where the parameter K is set to a value of five to produce an "over control" condition.

Reference 1: Mars Surveyor Program: 2001 Lander Mission Proposal Information Package, 30 June 1997

Reference 2: P. E. Moseley. "The Apollo Entry Guidance: A review of the mathematical development and its operational characteristics", TRW Note No. 69-FMT-791, December 1, 1969

Reference 3: Gerald L. Hunt. "Apollo Reentry Guidance and Navigation equations and flow logic", MSC Internal Note No. 65-FM-157, December 13, 1965

Reference 4: Claude A. Graves and Jon C. Harpold. "Apollo Experience report: Mission Planning for Apollo reentry", MSC Internal Note No. 70-FM-155, October 5, 1970

Reference 5: Arthur E. Bryson, Yu-Chi Ho, "Applied Optimal Control", Hemisphere Publishing Corporation, 1975.